Urban Climate 37 (2021) 100813

Contents lists available at ScienceDirect

Urban Climate

journal homepage: www.elsevier.com/locate/uclim

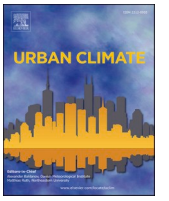

COVID-19 outbreak and air quality: Analyzing the influence of physical distancing and the resumption of activities in São Paulo municipality

Gregori de Arruda Moreira [a,b,*], Izabel da Silva Andrade [b], Alexandre Cacheffo [b,c], Alexandre Calzavara Yoshida [b,c], Antonio Arleques Gomes [b], Jonatan João da Silva [b,d], Fábio Juliano da Silva Lopes [b,e], Eduardo Landulfo [b]

[a] *Federal Institute of São Paulo (IFSP), Campus Registro. Avenida Clara Gianotti de Souza, 5180, Agrochá – CEP 11900-000, Registro, São Paulo, Brazil*

[b] *Center for Lasers and Applications (CELAP), Institute of Energy and Nuclear Research (IPEN), Avenida Lineu Prestes, 2242, Setor E5, Cidade Universitária – CEP 05508-000, São Paulo, São Paulo, Brazil*

[c] *Institute of Exact and Natural Sciences of Pontal (ICENP), Federal University of Uberlândia (UFU), Campus Pontal. Rua Vinte, 1600, Bloco C, Tupã – CEP 38304-402, Ituiutaba, Minas Gerais, Brazil*

[d] *Center for Exact Sciences and Technologies (CCET), Federal University of Western Bahia (UFOB), Campus Barreiras. Rua da Prainha, 1326, Morada Nobre – CEP 47810-047, Barreiras, Bahia, Brazil*

[e] *Department of Environmental Sciences, Institute of Environmental, Chemical and Pharmaceutical Sciences (ICAQF), Federal University of São Paulo (UNIFESP), Campus Diadema. Rua São Nicolau, 210, Centro – CEP 09913-030, Diadema, São Paulo, Brazil*

ARTICLE INFO

Keywords:
Automotive emissions
Remote sensing
Supervised machine learning
Air quality
Coronavirus

This work compares variations in the concentrations and air quality indexes of the pollutants PM_{10}, $PM_{2.5}$, CO, and NO_2, during the COVID-19 outbreak in São Paulo Municipality. Such comparisons considered the period of physical distancing (autumn) and the three first months of economic activities' resumption (winter). The concentrations and indexes observed in 2020 were compared with their correspondent values measured in the three preceding years. Also, from a supervised machine learning algorithm, the correspondent 2020 expected values were predicted and used in these comparisons. In order to analyze the influence of meteorological conditions, the seasons studied were characterized using remote sensing and surface data. The pollutants predominantly emitted by the vehicle fleet (CO and NO_2) had reductions in their concentrations, with values always below the predictions and good air quality indexes. However, the pollutants whose concentration is less dependent on automotive emissions (PM_{10} and $PM_{2.5}$) had high proximity to the predictions during the autumn and lower values during some periods in winter. This reduction was not enough to avoid days with a moderate air quality index. The approximation of the average concentrations of PM_{10}, $PM_{2.5}$, and CO to the prediction, from the second-half August

* Corresponding author at: Federal Institute of São Paulo (IFSP), Campus Registro. Avenida Clara Gianotti de Souza, 5180, Agrochá – CEP 11900-000, Registro, São Paulo, Brazil.

E-mail address: gregori.moreira@usp.br (G.A. Moreira).

https://doi.org/10.1016/j.uclim.2021.100813
Received 17 September 2020; Received in revised form 22 January 2021; Accepted 18 February 2021
Available online 22 February 2021

2020, indicates the influence of activities' resumption in air quality.

1. Introduction

In 2020, most countries and cities in the world had to undergo physical distancing measures to reduce the fast-spreading of COVID-19, an infectious disease caused by the new coronavirus SARS-CoV-2. In reason of the World Health Organization's (WHO) declaration that the COVID-19 outbreak is a pandemic and due to the high rates of disease contagion reported in several countries, São Paulo also went through a period of physical distancing.

The Metropolitan Region of São Paulo (MRSP), with around 21.5 million inhabitants, is one of the most populous regions globally, characterized by high demographic density, several industries, and vehicles (CETESB, 2019). Such an area comprises 39 cities and is divided into five minor regions: north, south, west, southwest, and central. This complex's main city is São Paulo, with around 12.8 million inhabitants (approx. 6% percent of Brazil's population) (IBGE, 2020). This city integrates all regions and encompasses more than half of the MRSP population and the higher automobile fleet (IBGE, 2020), the primary source of anthropogenic pollutants like CO, NOx, and Particulate Matter (CETESB, 2019).

At the beginning of March, São Paulo's State Government decreed some rules to reduce population infection rates (São Paulo Municipality, 2020). A partial lockdown closed non-essential services (restaurants, fitness centers, malls, theatres, and others). Only the essential services (supermarkets, drugstores, police stations, fire departments, and others) were able to operate, but with restrictions in the number of clients and a person-to-person distance. Offering public transportation was also reduced to stimulate the reduction of the people's circulation in the cities.

During the autumn period (March to May) of the partial lockdown, the physical distancing rate in the city of São Paulo varied between 45% and 59% (São Paulo Municipality, 2020), leading to a significant reduction in vehicle circulation (between 59% and 86%). The fleet of São Paulo corresponds to approximately 9.1 million vehicles (São Paulo Municipality, 2020). According to the 2018 Environment Company of São Paulo State (CETESB) Report, the vehicle fleet had a significant contribution in total emissions, in MRSP, of the following pollutants: PM_{10} (40%), $PM_{2.5}$ (37%), CO (97%), NO_X (64%), SO_X (17%) and, hydrocarbons (76%) (CETESB, 2019). Consequently, as the vehicles are the primary source of anthropogenic pollution in São Paulo city (Andrade et al., 2017), it is expected, therefore, a reduction in the concentration of pollutants like PM_{10}, $PM_{2.5}$, NO_2, and CO during this period.

Tobías et al. (2020), comparing the periods before and during the physical distancing, observed a significant reduction in NO_2 (45% to 51%) and PM_{10} (28% to 31%) concentration in Barcelona (Spain). Collivignarelli et al. (2020) performed a comparison of the variations in some pollutant concentrations before and during the partial lockdown in Milan (Italy), detecting a reduction of 57.6% and 47% in the concentrations of CO and NO_2, respectively. Otmani et al. (2020) observed in Salé (Morocco) reductions of 75% and 96% in the concentration of PM_{10} and NO_2, respectively, comparing the periods before and during the lockdown. Zalakeviciute et al. (2020), comparing the periods before and during the physical distancing in Quito (Ecuador), observed a reduction of 29% ($PM_{2.5}$), 38% (CO), and 68% (NO_2).

Although the physical distancing measures can reduce anthropogenic pollutant emissions, different meteorological conditions can positively influence the dispersion process, favoring the reductions in the pollutant concentrations (Stull, 1988). To reduce the possible effects of favorable meteorology, Sharma et al. (2020) performed a comparison between the concentrations of PM_{10}, $PM_{2.5}$, CO, and NO_2, in India, during the lockdown period and the same period of preceding years, finding a marked reduction mainly in the $PM_{2.5}$ concentration (around 43%). In the same way, performing comparisons with the preceding year, Dantas et al. (2020) identified a reduction in the concentrations of NO_2 (24.1% to 32.9%) and CO (37.0% to 43.6%) in Rio de Janeiro.

On 1 June 2020, São Paulo Municipality initiated the "Plano São Paulo," which enabled the resumption of some economic activities in the city (São Paulo Municipality, 2020). Such action resulted in a gradual decrease in the physical distancing rate and an increase in vehicle traffic. In this sense, this work compares the variations in the concentrations of PM_{10}, $PM_{2.5}$, CO, and NO_2 and the air quality indexes retrieved in four CETESB stations. Such a comparison intends to identify both the effects of the partial lockdown (occurred during autumn) and the resumption of economic activities (occurred during winter) in air quality and pollutant concentrations in the São Paulo Municipality.

Based on the database for the three preceding years' emissions, a machine learning technique was used to estimate the concentrations for all the pollutants mentioned above, considering a scenario without the outbreak. These estimates were then compared with the corresponding physical distancing rate variations and CETESB stations' retrievals in 2020. Moreover, from elastic lidar, rawinsonde, and surface sensors data, the winters and autumns from 2017 to 2020 were characterized and compared to analyze the influence of the atmospheric conditions.

This paper is structured as follows: in the second section, is given a brief description of the experimental site, instrumentation, and databases analyzed. Following this, the theory and methods employed to perform all the analyses are presented in the third section. The fourth section shows the results and discussion, where the results obtained are discussed in detail. Finally, in the last section, the conclusions are presented.

2. Instrumentation

2.1. Experimental site

São Paulo is characterized by a humid subtropical climate with a warm and humid summer, while winter is dry and with a not very large decrease in the average temperature. Spring and autumn have intermediate climatic characteristics, although March (the first

month of autumn) having high rainfall rates (CETESB, 2019).

Concerning environmental laws, the state of São Paulo has one of the strictest laws in Brazil. Since 2013, São Paulo has been looking to achieve the WHO's air quality standards (CETESB, 2020b). Since 2013 the government has changed the state environmental law of air quality, establishing three intermediate goals to gradually reduce the emission limits to reach a WHO's final standard (Paulo, 2013).

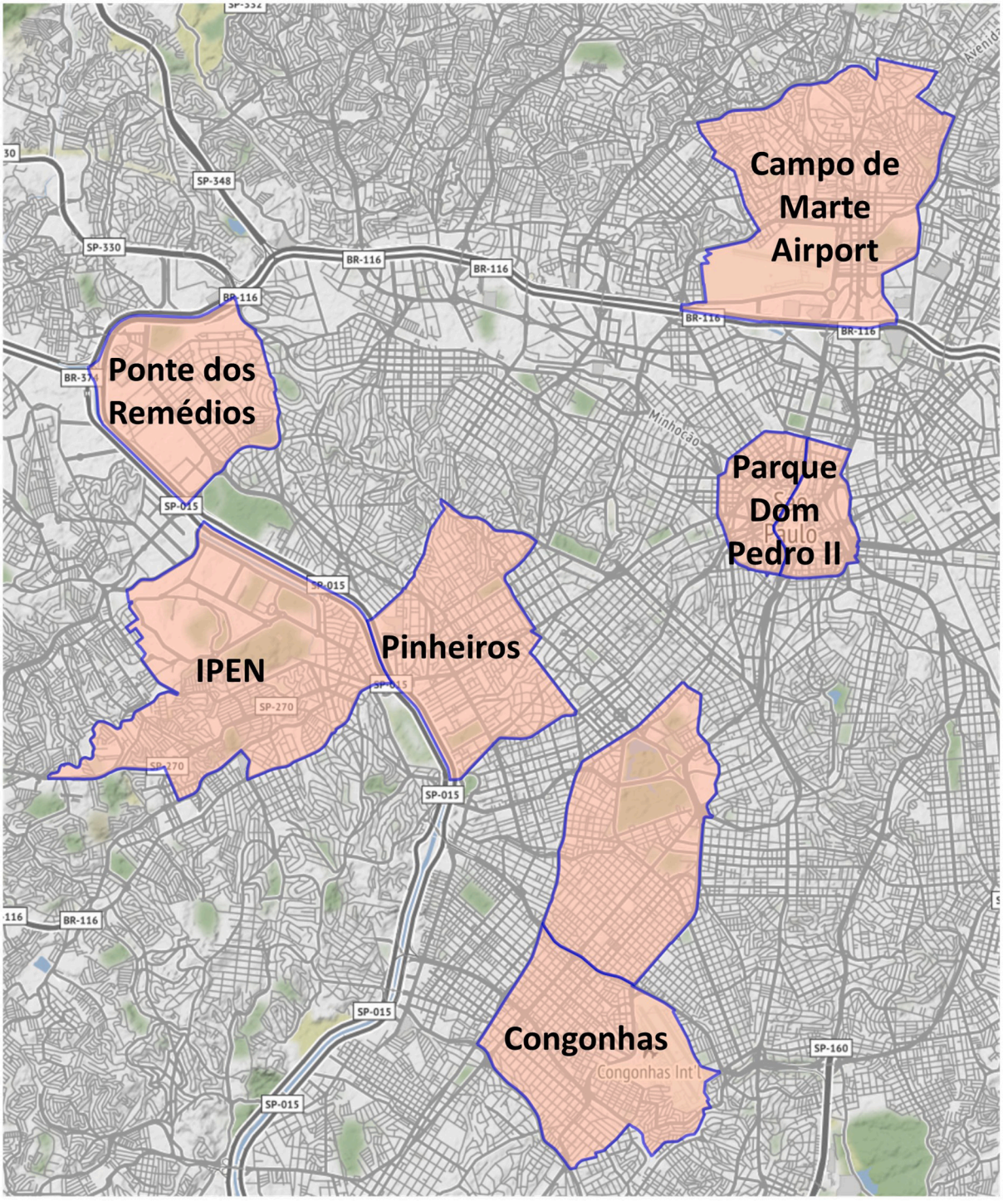

Fig. 1. Map of São Paulo's city, showing the districts where the four CETESB stations addressed in this work are placed. The locations of IPEN (Nuclear and Energy Research Institute), where the elastic lidar measurements were performed, and Campo de Marte Airport, where the rawinsondes launchings occur, are also shown.

As mentioned above, the measurements presented in this work were performed during autumn and winter from 2017 to 2020. The more restricted physical distancing, adopted due to the pandemic, was carried out between March and May 2020, a period corresponding to the autumn in the Southern Hemisphere, while the resumption of economic activities (Plano São Paulo) began in June 2020 (first month of winter in Southern Hemisphere). The data were collected from CETESB stations located in São Paulo, whose PM_{10}, $PM_{2.5}$, CO, and NO_2 data were available from 2017 to 2020. Such stations are: Congonhas (23° 36′57“ S, 46° 39’47” W), Parque Dom Pedro II (23° 32′42“ S, 46° 37’40” W), Pinheiros (23° 33′40“ S, 46° 42’06” W) and Ponte dos Remédios (23° 31′08“ S, 46° 44’35” W).

The Congonhas station is close to Congonhas Airport, the second busiest Brazilian airport with around 21.7 million passengers in 2018 (São Paulo Municipality, 2020), in the city’s southern region. A consequence of the proximity to the airport is that this region has heavy vehicle traffic. The Parque Dom Pedro II station stands in the city’s central area, near bus terminals, subway stations, and tourist attractions (São Paulo Municipality, 2020). The Ponte dos Remédios station is located in the northwest region of the city, close to the Marginal Tietê (officially, a section of the SP-015 highway). With a length of 24.5 km, it is the central expressway in the city, interconnecting the west, east, north, and central regions. Along this section of the SP-015 highway circulates 582 thousand light vehicles per day (São Paulo Municipality, 2020). The Pinheiros station is situated in the city’s western region, close to the Marginal Pinheiros (officially, another section of the SP-015 highway). With a length of 22.5 km, it is the second most significant expressway in the city, linking the north and south regions and interconnecting several other important highways and avenues. Along this section of SP-015 circulates 392 thousand light vehicles per day (São Paulo Municipality, 2020). Fig. 1 shows the approximate location of the four CETESB stations.

2.2. CETESB QUALAR platform and air quality index

CETESB operates 63 monitoring stations statewide, of which 17 are placed in the São Paulo Municipality. All the information and products derived from the measurements retrieved by these stations are available for download at the QUALAR Platform (CETESB, 2020a). The Air Quality Index (AQI) is a mathematical tool that delivers a dimensionless index for each pollutant, classifying the air quality accordingly to the value obtained (CETESB, 2020b). Both QUALAR Platform and AQI are mechanisms developed to improve the dissemination of data concerning air quality and meteorological information quickly and clearly for the population.

For all the analysis and comparisons performed in this work, the daily values for the concentration of the pollutants PM_{10}, $PM_{2.5}$, CO, and NO_2, and the AQI values (both obtained from the following CETESB stations Pinheiros, Parque Dom Pedro II, Congonhas, and Ponte dos Remédios) were retrieved from the tools above-mentioned for the periods indicated in the Introduction (during the partial lockdown (autumn) and the three first months of the resumption of economic activities (winter)). Additionally, the information about surface relative humidity (RH), surface temperature, and horizontal wind speed (HWS) were collected, with a temporal resolution of 1-h, from the Pinheiros station, which is the nearest to IPEN enabled to provide such parameters.

In São Paulo State, the classification of air quality has five indexes. Each one is labeled with a specific colour, ranging from the best scenario to the worst (CETESB, 2019). Fig. 2 presents these indexes.

2.3. SPU Lidar Station

The SPU Lidar Station is installed in the city of São Paulo (23°33′38”S, 46°44′23” W) at the Nuclear and Energy Research Institute

AQI	Index	PM_{10} ($\mu g.m^{-3}$) 24h	$PM_{2.5}$ ($\mu g.m^{-3}$) 24h	CO (ppm) 8h	NO_2 ($\mu g.m^{-3}$) 1h
N1 – Good	0 – 40	0 – 50	0 – 25	0 – 9	0 – 200
N2 – Moderate	41 – 80	>50 – 100	>25 – 50	>9 – 11	>200 – 240
N3 – Bad	81 – 120	>100 – 150	>50 – 75	>11 – 13	>240 – 320
N4 – Too Bad	121 – 200	>150 – 250	>75 – 125	>13 – 15	>320 – 1130
N5 – Terrible	>200	>250	>125	>15	>1130

Fig. 2. Patterns adopted by CETESB to classify the AQI values: N1 – Good, N2 – Moderate, N3 – Bad, N4 – Too bad, N5 – Terrible. The colors ranging from the best scenario to the worst are green, yellow, orange, red, and purple. (For interpretation of the references to colour in this figure legend, the reader is referred to the web version of this article.)

(CELAP/IPEN). It has been monitoring the optical properties and vertical distribution of aerosols since 2001 using an elastic lidar system, which operates in the coaxial mode. The lidar works with a pulsed Nd:YAG laser, emitting radiation at wavelengths 355, 532, and 1064 nm, with a repetition rate of 10 Hz and pointing to zenith direction. The detection is performed at three elastic channels (355, 532, and 1064 nm) and three Raman-shifted channels (387, 408, and 530 nm). This system works with a temporal and spatial resolution of one minute and 7.5 m, respectively, reaching the full overlap at 300 m, a.g.l (Moreira et al., 2019). For this work, all lidar measurements were obtained from the wavelength of 532 nm (elastic).

2.4. Rawinsonde retrievals and rainfall data

In São Paulo's city, two rawinsondes are launched daily, at 09:00 and 21:00 Local Time, from the Campo de Marte Airport (23°30′33" S, 46°38'12" W). Fig. 1 shows the approximated localization of the airport. In this paper, the rawinsonde were obtained from the University of Wyoming website (http://weather.uwyo.edu/upperair/sounding.html). Only the launches performed at 09:00 Local Time were considered.

The rainfall data were retrieved from the Mirante de Santana station (23°29′47" S, 46°37'12" W), operated by the National Institute of Meteorology (INMET). The Mirante de Santana station is placed close to Campo de Marte Airport (INMET, 2020).

3. Theory and methods

3.1. Observation of the atmospheric boundary layer cycles

The lowermost troposphere region is the Atmospheric Boundary Layer (ABL). Such a layer has turbulent (mechanical and thermodynamic) characteristics, which give it great importance in Environmental Sciences, mainly in matters related to air quality and pollutant dispersion (Moreira et al., 2020). The ABL has a daily cycle (directly associated with its stability), in a way that it subdivides into three main sublayers: Convective Boundary Layer (CBL), nocturnal Stable Boundary Layer (SBL), and Residual Layer (RL). The SBL forms at night due to the radiative cooling of the ground. In this layer, which is hotter than the underlying surface, the turbulence mixing is suppressed. The SBL layer is covered by the RL, which is endowed with intermittent turbulence, and it is not affected by the turbulence transport from the surface. Such a layer remains at the same height as the maximum reached by the CBL of the preceding day. Until few instants before sunrise, SBL and RL coexist. However, after this, the ground becomes warm, and the heat transfer process starts, generating convective thermals, which cause turbulent mixing. Then, the CBL substitutes the SBL and rises during the day, breaking the RL and achieving the maximum at around the middle of the day (Stull, 1988). Measurements performed by two different instruments – elastic lidar (between 10:00 and 18:00 LT) and rawinsonde (09:00 LT) – were analyzed to estimate and observe the ABL cycles more broadly.

3.2. Estimation of the convective boundary layer height from Lidar measurements and Rawinsonde retrievals

The lidar measurements were performed from 10:00 to 18:00 LT to estimate the CBL height (CBLH). All lidar results were obtained from the wavelength 532 nm after utilizing the three-step correction (D'Amico et al., 2016). In the first step of this correction, to reduce the influence of the electrical noise, the dark current signal ($DC(z)$) is subtracted from the raw signal ($P(z)$). Then, to attenuate external sources' influence, the background radiation signal (BG) is removed. Finally, because of the signal's attenuation with the height, the two early steps' value is multiplied by the square of the corresponding height. From such actions is obtained the Range Corrected Signal (RCS_{532}), as indicated in the equation below:

$$RCS_{532}(z) = (P(z) - DC(z) - BG)\, z^2 \tag{1}$$

After the three-step correction, the CBLH was estimated from the Wavelet Covariance Transform Method (WCT) (Baars et al., 2008). In this method is performed a covariance (W) between the average $RCS_{532}(z)$ obtained during one hour ($\overline{RCS_{532}}(z)$) and a mother-wavelet which is given, in this case, by the Haar function ($h\left(\frac{z-b}{a}\right)$). In this way, we have the expression for the covariance:

$$W(a,b) = \frac{1}{a}\int_{z_i}^{z_f} \overline{RCS_{532}}(z)\, h\left(\frac{z-b}{a}\right) dz \tag{2}$$

where a and b are respectively the values of dilatation and transition-related to mother-wavelet, z is the height above the ground, and z_i and z_f are the respective lower and upper limit of the $\overline{RCS_{532}}(z)$. Finally, the CBLH is identified from the maximum in the covariance profile:

$$CBLH = Max(W(a,b)) \tag{3}$$

which corresponds to the sharpest drop in the $\overline{RCS_{532}}(z)$ and, consequently, to a high reduction in the aerosol concentration or, in other words, the transition between the ABL and the Free Troposphere (Baars et al., 2008).

From the rawinsonde retrievals at 09:00 LT, the CBLH was obtained by the Parcel Method (Holzworth, 1964), which, by the potential temperature profile, estimates the height from the ground where the parcel of air with ambient temperature can rise

adiabatically, by the convective process. The RL height (RLH) was estimated from the higher gradient in the potential temperature profile above the CBLH (Moreira et al., 2021).

3.3. Ventilation coefficient calculation

Towards identifying the rate at which air within the CBL is transported away from a determined region, the Ventilation Coefficient (VC) is calculated by multiplying the CBLH and the horizontal wind speed (HWS) (Moreira et al., 2020; 2021). To standardize all variables' temporal resolution, the VC is calculated from the one-hour average of the horizontal wind speed ($\overline{HWS}$):

$$VC = CBLH \cdot \overline{HWS} \tag{4}$$

The CBLH estimated from rawinsonde represents only an instant in the time series, while the values estimated by lidar measurements represent an average of one hour. Therefore, the VC was calculated only with CBLH obtained from lidar measurements (10:00 to 18:00 LT).

3.4. Thermal inversions

In the troposphere, the temperature has a positive vertical gradient. However, in some situations, the ground can lose heat rapidly at night, and the air in contact with the surface cools. Then, the warmer air masses ascend, trapping the colder air close to the ground, causing a negative gradient in the vertical temperature profile (Stull, 1988). Such a phenomenon is called thermal inversion. The thermal inversion can confine pollutants in the region below it, attenuating convective processes and making it difficult for the dispersion process. In this paper, the thermal inversions were obtained from the temperature profile of rawinsonde retrievals (at 09:00 LT) and classified into three ranges: below 200 m, between 200 m and 500 m, and above 500 m.

3.5. Prediction of pollutants concentrations

Predictions for the concentrations of the four pollutants analyzed in this paper ($PM_{2.5}$, PM_{10}, CO, and NO_2) were performed using Sktime: a Python library for machine learning (Löning et al., 2019). It was applied a supervised technique from an exponential smoothing model (Hynddman and Athanasopoulos, 2014).

The three years data (the average daily pollutants concentrations for the four CETESB stations considered in this paper) were divided into two groups: training (used to train the model) and test (applied in the validation of the model). The model generated provides us with an accuracy of 90.1% (PM_{10}), 89.7% ($PM_{2.5}$), 90.7% (CO), and 91.0% (NO_2).

4. Results and discussion

4.1. Analysis of meteorological variables

Fig. 3 presents the average hourly values of surface temperatures and RH for the autumns of 2017–2019 (blue and red dots, respectively) and 2020 (navy and orange dots, respectively) retrieved by Pinheiros station. The shadows indicate the standard deviation for the data between 2017 and 2019. The surface temperature in 2020, during the dawn and early morning, is approximately 2.5 °C lower than the average values for 2017–2019. Between 14:00 and 17:00 LT, the average of 2020 values is closer than the average for 2017–2019. The maximum average value observed in 2020 is displaced by one hour about the average value observed between 2017 and 2019. RH's average hourly values in 2020 present the majority lower values than those for 2017–2019, mainly in the afternoons. Therefore, the data show that autumn 2020 can be considered colder and drier when considering the average hourly values

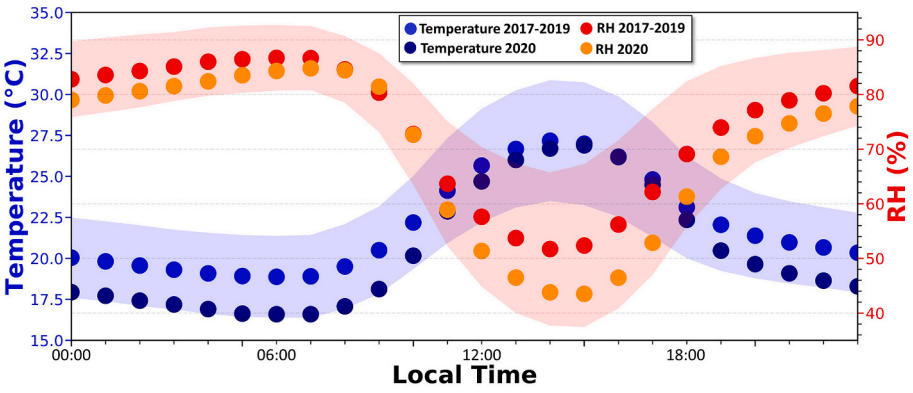

Fig. 3. Average hourly values of the surface temperature and RH, obtained during the autumn in the CETESB Pinheiros station.

compared with the preceding three years.

Table 1 shows a comparison between the average rainfall rates in the autumn months of 2017–2019 and 2020. In all months of autumn 2020, the rainfall rates are much lower than the average values registered in the corresponding months for the preceding three years.

Fig. 4-a shows the values of CBLH (estimated from elastic lidar measurements and rawinsonde retrievals) and RLH. The RL maintains in 2020 an average value close to that one observed in 2017–2019. On the other hand, the CBLH daily evolution presents higher values in 2020, during the three first hours, and lower values from 13:00 to 18:00 LT. Moreover, such information indicates lower values of the CBL growth rate and duration in autumn 2020 compared to the same season in 2017–2019. Even though the average values observed between 10:00 and 12:00 Local Time for autumn 2020 are higher than those of 2017–2019 (as a consequence of the CBLH and HWS behavior during autumn 2020), the VC (Fig. 4-b) has average values predominantly lower than those observed during 2017–2019, mainly the value corresponding to the maximum for 2017–2019, which occurs at 15:00 LT.

Table 2 presents the numbers of thermal inversions in the autumn months of 2017–2019 and 2020. Considering the values of the CBLH at 09:00 LT, the number of thermal inversions observed above such height is around 45% higher in 2020 compared to the average values of 2017–2019. In the region below the CBLH, the unique difference is observed below 200 m, where the number in 2020 (three) is higher than the average value of 2017–2019 (two). It must be mentioned that thermal inversions are a recurring problem related to pollutants dispersion in São Paulo throughout autumn and especially in winter (Andrade et al., 2017).

Therefore, it is possible to conclude from this analysis that autumn 2020 is drier, colder, and has lower CBLH and VC average values than the three preceding years (2017–2019). In addition to this, the number of thermal inversion events above CBLH at 09:00 LT is higher in 2020. Therefore, autumn 2020 had less favorable conditions for pollutants dispersion than the average for the same period in the preceding three years.

Similar to Fig. 3, Fig. 5 presents the values of surface temperature and RH; however, it is focused on winter. The surface temperature values observed in 2020 are slightly higher than those observed during 2017–2019. The RH observed in 2020 is slightly lower than the values observed during 2017–2019, mainly between 11:00 to 19:00 Local Time.

The rainfall rate (Table 3) observed in June 2020 is three times higher than the average of the last three years for the same month. August 2020 also had a rainfall rate higher than the average. On the other hand, July 2020 had values below the average observed in 2017–2019.

The average RLH observed in winter 2020 (Fig. 6-a) is higher than the values observed between 2017 and 2019. Similarly, the average CBLH daily cycles (Fig. 6-a) are predominantly higher than those observed in 2017–2019, mainly between 12:00 and 16:00 Local Time. Such characteristics enable the higher values of VC observed in winter 2020 compared with winter 2017–2019 (Fig. 6-b).

Regarding the thermal inversions in winter (Table 4), the behavior observed in 2020 is similar to 2017–2019 in the CBL region. In the RL region, there is an increase of 1 occurrence. Thus, winter 2020 can be characterized as wetter and hotter compared to the period 2017–2019. Besides, in 2020, higher average CBLH and VC values were observed between 12:00 and 16:00 Local Time. Such characteristics favor the pollutant dispersion process.

4.2. Analysis of the measured pollutants concentrations

Fig. 7 presents a comparison between the average concentrations of the pollutants PM_{10}, $PM_{2.5}$, CO, and NO_2 in autumn 2020 (during the partial lockdown) and autumn 2017–2019.

Fig. 7-a presents the variation for the pollutant PM_{10}. A more significant reduction in PM_{10} concentration was observed in Pinheiros station (24.8–22.0 $\mu g.m^{-3}$ [around −11%]), where two months (March and April) of measurements were performed. On the other hand, Ponte dos Remédios and Congonhas stations had an increase in the average concentration (Ponte dos Remedios (29.3–29.7 $\mu g.m^{-3}$ [around +1%]), Congonhas (27.8–28.3 $\mu g.m^{-3}$ [around +2%]). In this last case, the less favorable conditions observed and the high contribution (around 60%) of other PM_{10} emitting sources in the MRSP may cause these effects to pollutants dispersion observed in 2020 compared with the three preceding years.

Fig. 7-b presents the variation for the pollutant $PM_{2.5}$. In the same way, as observed for the pollutant PM_{10}, a more significant reduction of $PM_{2.5}$ was detected in Pinheiros station (16.0–13.0 $\mu g.m^{-3}$ [around −18.7%]), where one month (March) of measurements was performed. Such reduction can be associated with a decrease in the light-vehicle fleet, which is the primary pollutant source. Ponte do Remédios station had the lowest reduction (17.5–16.7 $\mu g.m^{-3}$ [around −4%]). However, this station has a higher average concentration value because the expressway in its vicinity (SP-015 road) connects several regions of the city. The intense traffic of essential service vehicles in the SP-015 road, combined with less favorable conditions to pollutants dispersion (compared to the three preceding years), may have contributed to this lower reduction.

In Fig. 7-c, considering the pollutant CO, the highest and lowest decreases were observed in Parque Dom Pedro II (0.41–0.27 ppm

Table 1
Average rainfall rates in autumn months of 2017–2019 and 2020.

		Rainfall Rate (mm)	
Season	Month	2017–2019	2020
Autumn	March	161.0	64.0
	April	82.0	6.8
	May	78.0	8.4

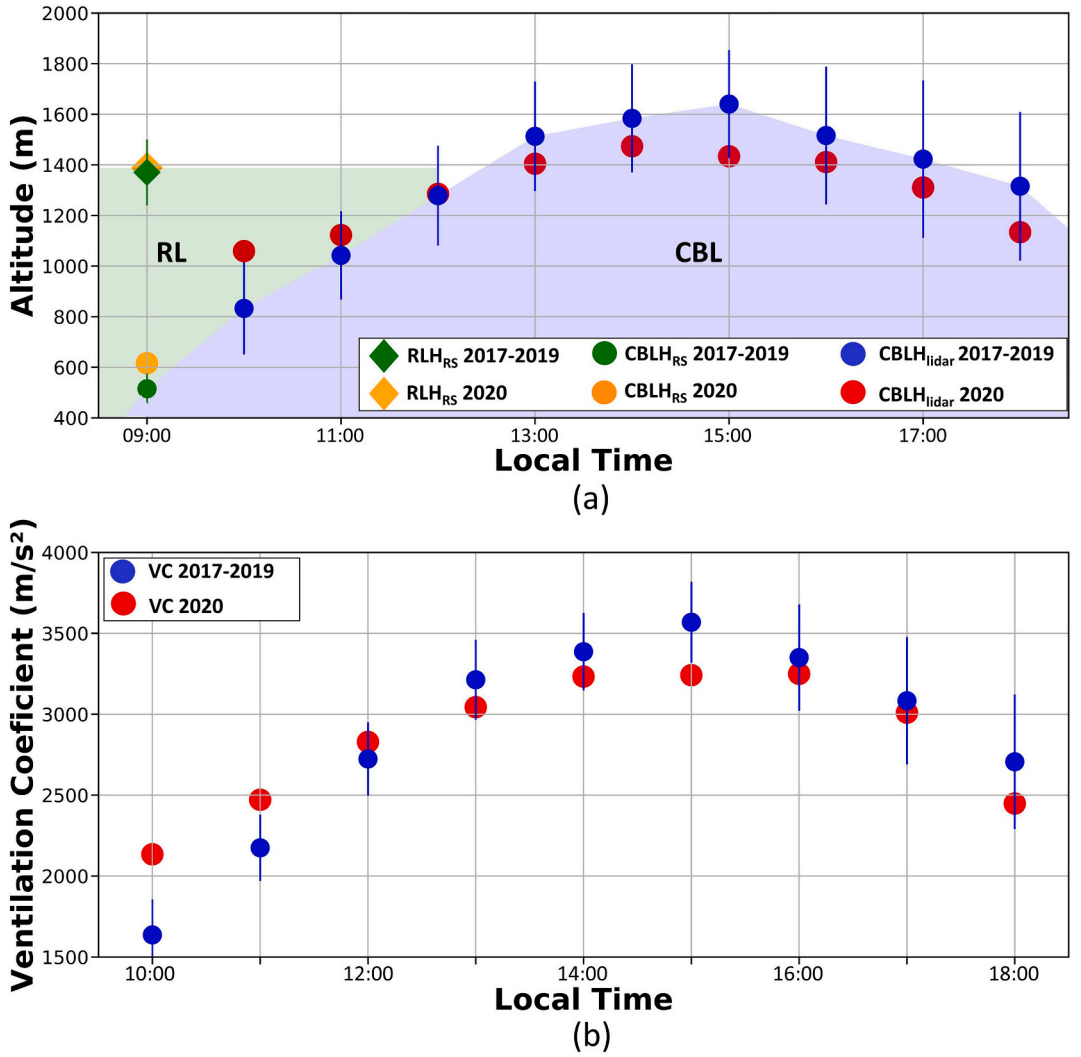

Fig. 4. (a) Average hourly values of the CBLH and RLH estimated from elastic lidar and rawinsonde data for autumns 2017–2019 and 2020. (b) Average ventilation coefficient values, calculated for autumns 2017–2019 and 2020.

Table 2
Thermal inversions per region.

	Number of thermal inversions		
Height Seasons	< 200 m	200-500 m	> 500 m
Autumn (2017–2019)	2	9	22
Autumn (2020)	3	9	28

[around −34.1%]) and Pinheiros (0.50–0.37 ppm [around −26%]) stations, respectively. The concentration for the pollutant NO_2 presented in Fig. 7-d had a significant reduction in Pinheiros station (38.0–23.0 μg.m^{-3} [around −39%]), expected due to considerable reductions in the vehicle fleet in this region. The lowest variation was observed in the Congonhas station (53.8–49.6 μg.m^{-3} [around −7%]), the area with the highest average values. This lowest variation was already expected because, as mentioned in Section 2.1, this station is situated next to the airport, where heavy vehicle traffic occurs. Between March and April, Krecl et al. (2020) observed a reduction of NO_2 in 13 CETESB stations situated in the MRSP. The most considerable decreases were observed in Congonhas, Pinheiros, and Ponte dos Remédios stations.

Considering the four stations analyzed, it is possible to observe the effect of partial lockdown in the variation of the pollutants PM_{10}, $PM_{2.5}$, CO, and NO_2. The majority of negative variations were observed in Pinheiros (which has the vehicle fleet as the primary anthropogenic source). Excepting the CO, all pollutants concentration had lower variations in the regions where the higher average-

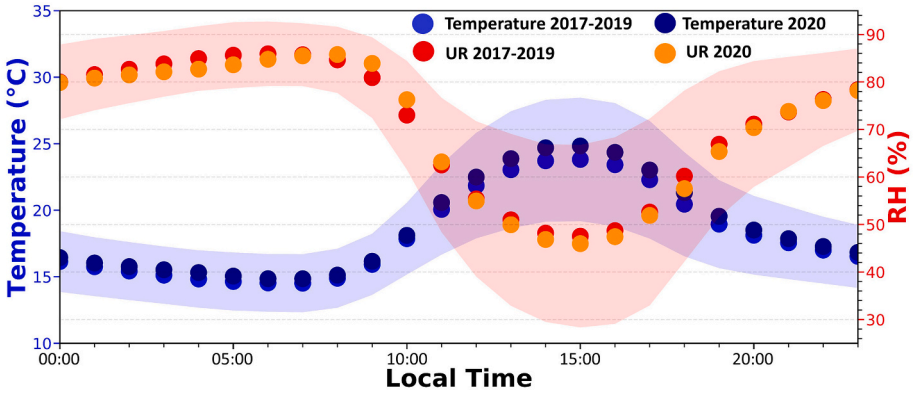

Fig. 5. Average hourly values of the surface temperature and RH obtained during winter in the CETESB Pinheiros station.

Table 3
Average rainfall rates in winter months of 2017–2019 and 2020.

		Rainfall Rate (mm)	
Season	Month	2017–2019	2020
Winter	June	50.0	150.4
	July	48.0	11.6
	August	30.0	65.4

values were observed. Similar results also were observed by Debone et al. (2020), which indicate a reduction in PM_{10}, $PM_{2.5}$, and NO_2 concentration in São Paulo city during the autumn period, so that, in the same way as presented in Fig. 7-c, the higher reductions are related to NO_2 concentration. Nakada and Urban (2020), using data from the Tropospheric Monitoring Instrument (TROPOMI) on-board Sentinel-5P satellite, also observed an intense reduction in NO_2 concentration between March and April (autumn).

Although economic activities have not been fully re-established, the partial resumption, combined with winter atmospheric characteristics, resulted in a higher concentration of $PM_{10,}$ $PM_{2.5}$, CO, and NO_2 during winter 2020 (Fig. 8) compared to autumn 2020.

Fig. 8-a presents the variation for the pollutant PM_{10}. A more significant reduction in PM_{10} concentration was observed in the Congonhas station (37.4–33.3 $\mu g.m^{-3}$ [around −11%]). In contrast, Pinheiros station increased the average concentration (34.8–35.7 $\mu g.m^{-3}$ [around +2%]). The main sources of PM_{10} in the city of São Paulo are secondary aerosols, resuspension, and industrial process, which together have a contribution of around 60% (CETESB, 2020c). Therefore, such sources can have significantly affected the concentration in the Pinheiros station. On the other hand, Congonhas airport is situated close to 23 May Avenue, the road with the highest vehicle traffic in São Paulo (CET, 2020a). However, as the airport still has restrictions in its activities, the number of vehicles in this region is considerably low compared to the values observed in the preceding years (CET, 2020b).

The concentration of $PM_{2.5}$ decreased in the four CETESB stations, as seen in Fig. 8-b. The highest decrease was observed in the Ponte dos Remédios station (27.8–22.0 $\mu g.m^{-3}$ [around −21%]), while the lowest reduction was detected in the Parque Dom Pedro II station (22.0–18.3 $\mu g.m^{-3}$ [around −17%]).

In the same way as $PM_{2.5}$, the CO concentration (Fig. 8-c) was also reduced in all analyzed stations. The higher reduction was observed in the Pinheiros station (0.82–0.63 ppm [around −23%]), while the lower one was detected in the Ponte dos Remédios station (0.90–0.80 ppm [around −11%]).

Fig. 8-d presents the concentration for the pollutant NO_2. The Pinheiros station had a higher reduction (49.8–33.7 $\mu g.m^{-3}$ [around −32%]). On the other hand, the Ponte dos Remédios station had a lower variation (68.7–65.0 $\mu g.m^{-3}$ [around −2%]).

The lower reductions of CO and NO_2 in the Ponte dos Remédios station reveal the influence of the resumption of activities because the road close to this station interconnects several regions of the MRSP. On the other hand, as already mentioned, the Pinheiros station (where the higher variations in the concentrations of CO and NO_2 were observed) is situated near a road that interconnects two critical regions of the city (the second road with the highest traffic in the city (CET, 2020a)). Consequently, although the partial activities resumption, the vehicular traffic is not comparable with the numbers observed in the preceding years, resulting in lower CO and NO_2 concentrations. It is also essential to observe that the negative variations of CO and NO_2 (which have the vehicle fleet as the primary source) were lower in winter than in autumn.

4.3. Analysis of the predicted pollutants concentrations

In order to analyze the influence of the physical distancing rate on the average concentration of each pollutant observed in the four stations of CETESB, such variables were compared with the expected average concentrations values (which were obtained through machine learning techniques, as described in section 3.5).

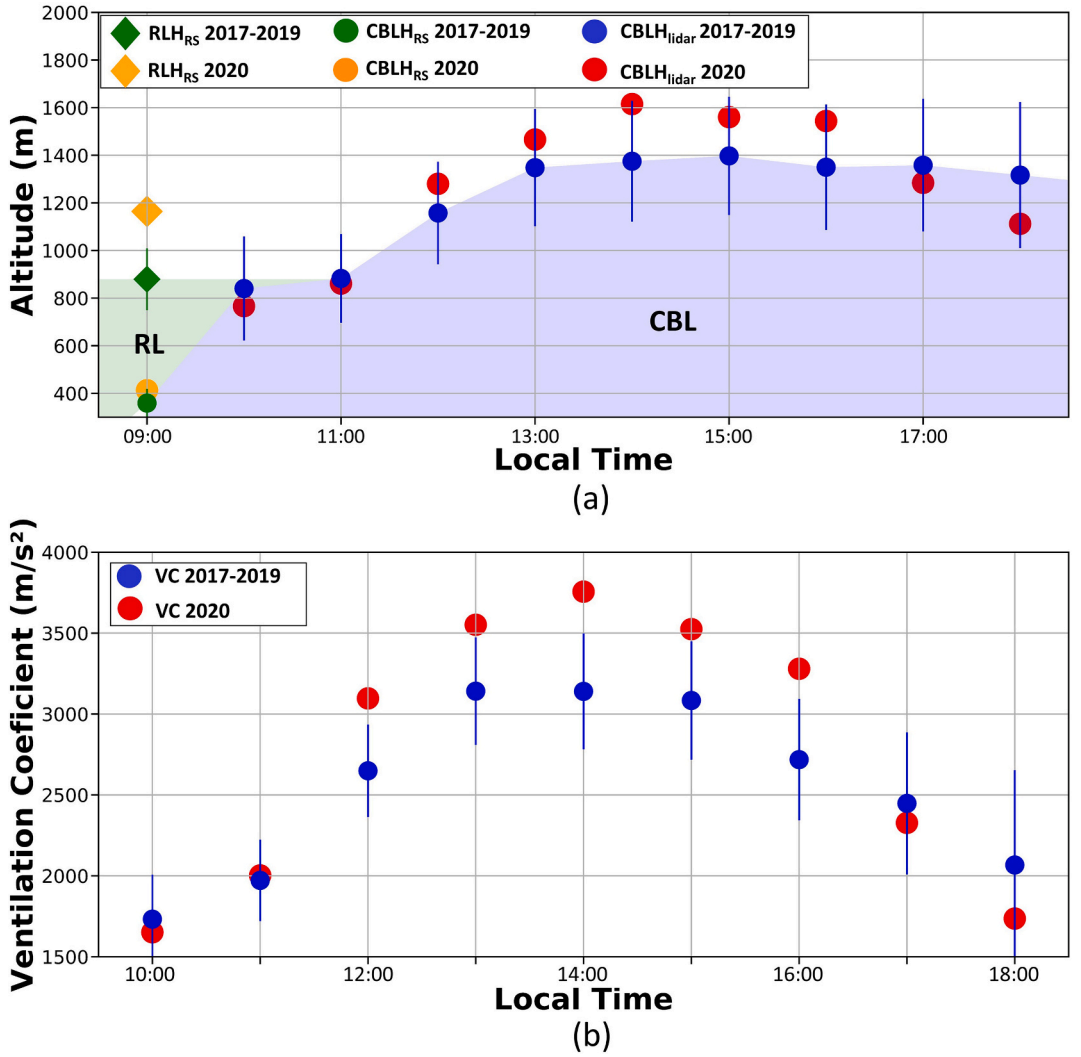

Fig. 6. (a) Average hourly values of the CBLH and RLH estimated from elastic lidar and rawinsonde data retrieved for winters 2017–2019 and 2020. (b) Average ventilation coefficient values estimated for winters 2017–2019 and 2020.

Table 4
Thermal inversions per region.

	Number of thermal inversions		
Height Seasons	< 200 m	200-500 m	> 500 m
Winter (2017–2019)	7	9	25
Winter (2020)	6	10	27

Fig. 9 presents the measured (blue line) and predicted (dashed black line) weekly average values of concentration of the pollutants covered in this paper. The black shadows represent the uncertainties of the prediction model, and the red line the average value of the Physical distancing rate. The green vertical bars represent the weekends so that it is possible to observe their effects on the physical distancing rate and the daily values of the pollutants' concentration (these two variables are inversely proportional).

In Fig. 9-a and 9-b, during autumn, PM_{10} and $PM_{2.5}$ measured values are close to the predicted ones and follow Fig. 7, which shows less reduction of these pollutants. However, in winter, a higher increase was expected, especially between July and August, which was not observed, as indicated in Fig. 8. The higher average values of VC and rainfall rate observed in winter 2020 affected the dispersion of PM_{10} and $PM_{2.5}$ positively. Although the vehicle fleet is not the primary source of such pollutants in São Paulo city, the physical distancing rate (albeit decreasing) combined with the meteorological conditions resulted in the lower concentrations of PM_{10} and $PM_{2.5}$, in comparison with predicted values, mainly in August.

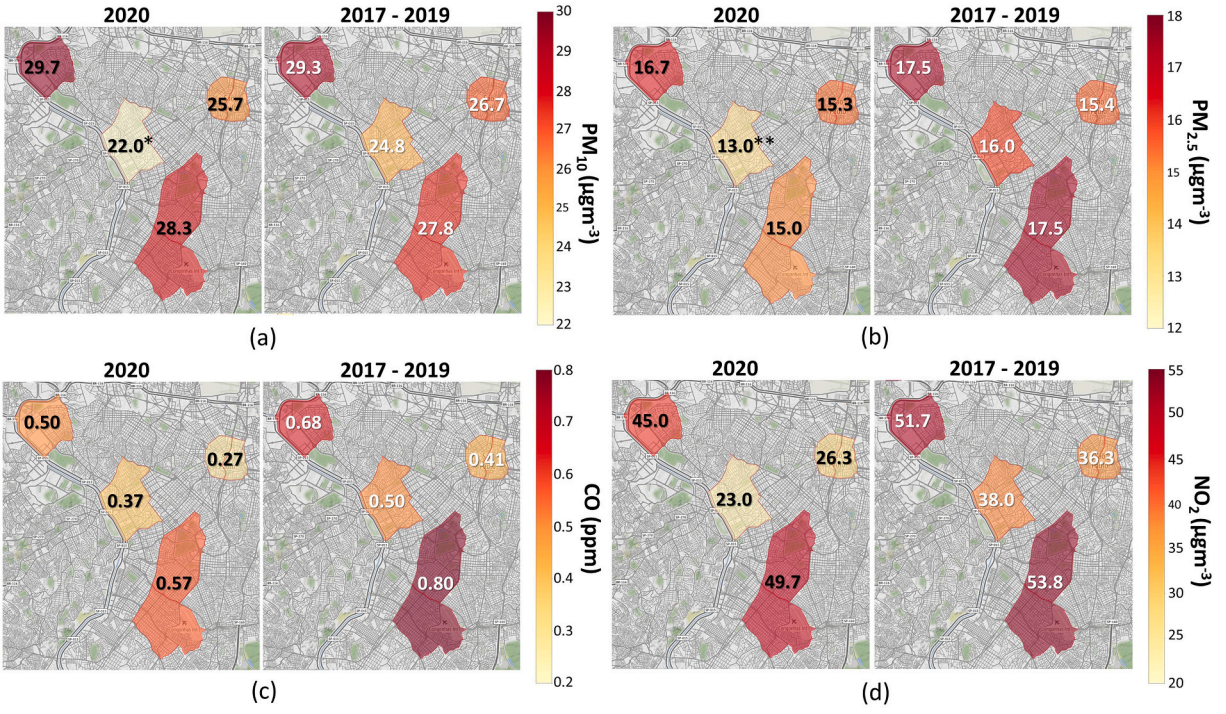

Fig. 7. Concentrations of the pollutants (a)PM_{10}, (b)$PM_{2.5}$, (c)CO, and (d)NO_2 in autumn 2020 (during the partial lockdown) and autumn 2017–2019 (average).

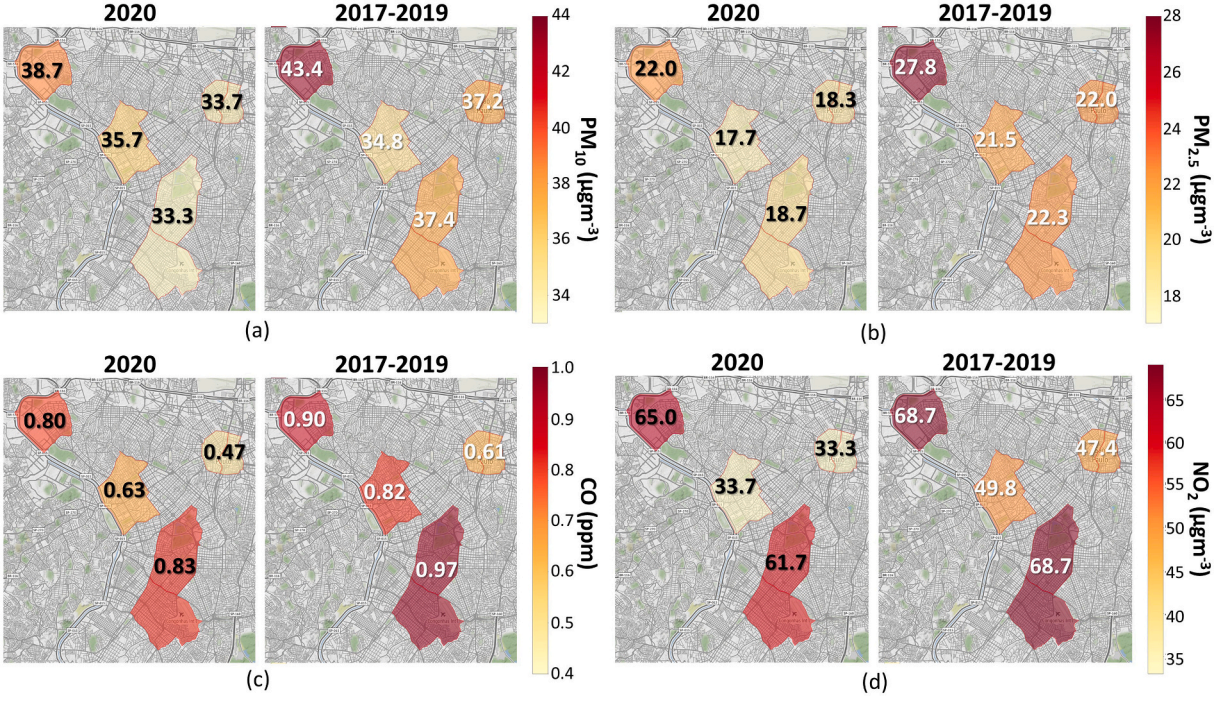

Fig. 8. Concentrations of the pollutants (a) PM_{10}, (b) $PM_{2.5}$, (c) CO, and (d) NO_2 in winter 2020 (three first months of resumption of the economic activities) and winter 2017–2019 (average).

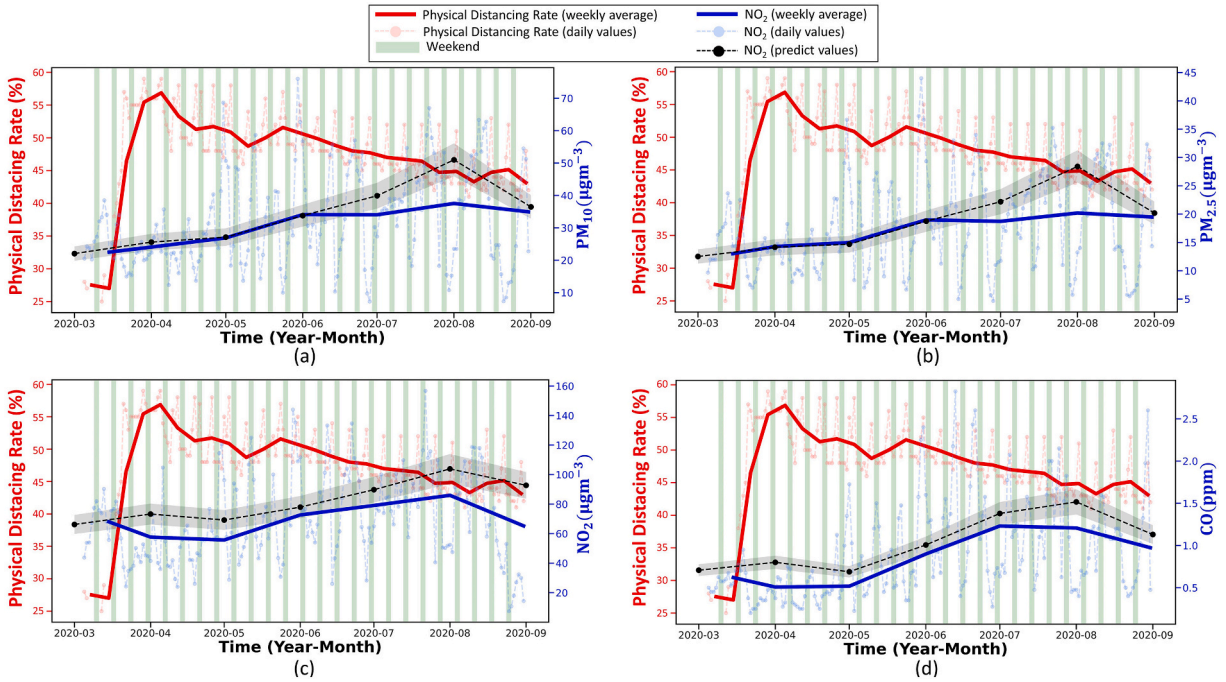

Fig. 9. Comparison among the physical distancing rate (red line) and the concentrations of the pollutants (a) PM_{10}, (b) $PM_{2.5}$, (c) CO, and (d) NO_2 predicted (black dotted lines) and measured (blue line) between March to August winter 2020. (For interpretation of the references to colour in this figure legend, the reader is referred to the web version of this article.)

On the other hand, in Fig. 9-c and 9-d, the values measured are always lower than the predicted, following Figs. 7 and 8. It is fundamental to highlight that NO_2 and CO have the vehicle fleet as the primary source. Consequently, they are more affected by the physical distancing rate. However, since June, the physical distancing rate had begun to decrease. Although the concentration of these pollutants increased (NO_2 in June and July; CO in June), it remained below the predicted values, with a significant reduction in August. Therefore, although the physical distancing rate is declining, the meteorological conditions helped pollutant concentration values continue below the predicted one.

Excepting the NO_2, which was the pollutant more affected by physical distancing, the measured values became increasingly closer to those predicted from the second half of August. This characteristic, associated with a gradual reduction in physical distancing rate, indicates a tendency to return to the pollutant concentration pattern observed before the pandemic.

4.4. Analysis of the AQI classifications

Fig. 10 presents a comparison between the AQI classifications considering the four pollutants analyzed in this work: in the three preceding autumns and winters and during these same seasons in 2020.

Analyzing the AQI classifications for the Pinheiros station, presented in Fig. 10-a, among the pollutants observed in this work, PM_{10} and $PM_{2.5}$ showed more variability, so that the best condition was observed in autumn 2020. Fig. 10-b shows the AQI classifications for the Parque Dom Pedro II station. Excepting PM_{10}, which had worse results in autumn 2020, all pollutants improved AQI during autumn and winter 2020.

Congonhas station (Fig. 10-c) did not show a variation in the AQI of $PM_{2.5}$ during autumn 2020, resulting from the less favorable conditions to pollutant dispersion indicated in Section 4.1. However, during winter, the AQI of all pollutants, except CO, improved, mainly to PM_{10} and $PM_{2.5}$. Ponte dos Remédios station (Fig. 10-d) had worse AQI for PM_{10} and $PM_{2.5}$, during autumn 2020, probably due to meteorological conditions. On the other hand, during winter, both pollutants had an increase in the AQI.

The results presented show that the variations observed in the AQI classifications were more significantly positive to pollutants predominantly emitted by the vehicle fleet (CO and NO_2). On the other hand, the pollutants whose concentration is less dependent on automotive emissions (PM_{10} and $PM_{2.5}$) maintained the same pattern or increased the number of days with AQI classification as moderate or good. In addition, it is also fundamental to emphasize that the reductions in these pollutants' concentrations were not enough to avoid days with AQI as moderate. Connerton et al. (2020) also observed a higher influence of partial lockdown in pollutants' concentration whose vehicle fleet is the primary source.

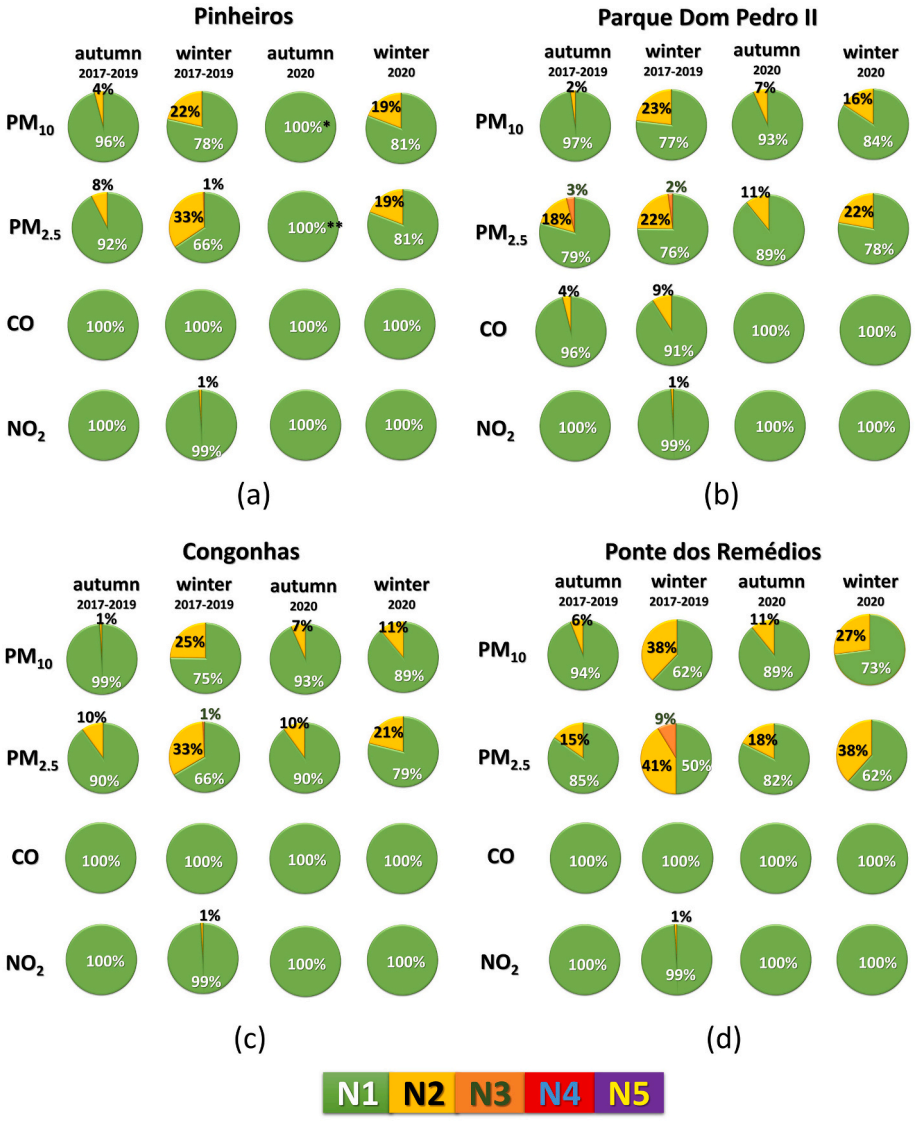

Fig. 10. CETESB AQI classification for the pollutants PM_{10}, $PM_{2.5}$, CO, and NO_2, in the three preceding autumns and winters (2017–2019) and during these same seasons in 2020.

5. Conclusions

This paper compares the concentration values (measured and predicted) and AQI classifications for PM_{10}, $PM_{2.5}$, CO, and NO_2 pollutants in the period during the lockdown (autumn) and in the first three months of the resumption of economic activities (winter) in four CETESB stations placed in São Paulo Municipality. To reduce possible effects of the influence of meteorological conditions, a comparison among measurements of relevant variables (CBLH, RLH, VC, number of thermal inversions, surface temperature, and humidity concentrations) in autumn and winter 2020, and their average values obtained for the three preceding years, was performed.

Regarding the meteorological conditions, it was possible to observe less favorable conditions to pollutant dispersion in autumn 2020 than in 2017–2019. On the other hand, higher values of VC and rainfall rates were observed in winter 2020, compared with 2017–2019, which can favor the pollutant dispersion process.

Concerning the concentration, the pollutants more dependent on the vehicle emissions (NO_2 and CO) presented the most considerable variations, with the measured values always lower than the predicted ones. Such variations occurred principally in winter: although the physical distancing rate in winter was lower than in autumn, weather conditions can have favored the dispersion process. Also, these pollutants had all days with AQI classification as good in autumn and winter 2020.

On the other hand, the pollutants less dependent on automotive emissions (PM_{10} and $PM_{2.5}$) presented lower variations than NO_2 and CO. In autumn, the values observed are similar to predict ones. However, in winter, the measured values are lower than those

predicted, suggesting that the combination of partial lockdown and meteorological conditions favored the reduction in the pollutant concentrations. Nevertheless, this reduction was not enough to avoid days with AQI classification as moderate.

The pandemic situation and the transition of partial lockdown to the resumption of economic activities provided a valuable experiment about the vehicle fleet's influence on the air quality. The observed results can shed light on possible improvements in public policies related to sustainable urban mobility because a reduction in vehicular traffic can significantly impact air pollution mitigation.

In conclusion, the variations observed in AQI classifications and the pollutant concentrations clarify the effects due to the reduction of the vehicle fleet, which was more effective in the pollutants where the vehicular emission is the primary source. The resumption of economic activities indicates, as expected, a tendency to return to the pollutant concentration pattern observed before the pandemic and predict by the model.

Declaration of Competing Interest

The authors declare that they have no known competing financial interests or personal relationships that could have influenced the work reported in this paper.

Acknowledgments

The authors are thankful to CETESB for providing data through the QUALAR database, the INMET for providing data about the rainfall rates and, the University of Wyoming for providing the rawinsonde retrievals database. We also acknowledge the National Council for Scientific and Technological Development (CNPQ) for their support on project 432515/2018-6 and the Coordination for the Improvement of Higher Education Personnel (CAPES) for the following scholarships: 88887.464990/2019-00, PROEX 88887.595780/2020-00.

References

Andrade, M.F., Kumar, P., Freitas, E.D., Ynoue, R.Y., Martins, J., Martins, L.D., Nogueira, T., Perez-Martinez, P., Miranda, R.M., Albuquerque, T., Gonçalves, F.L.T., Oyama, B., Zhang, Y., 2017. Air quality in the megacity of São Paulo: evolution over the last 30 years and future perspectives. Atmos. Environ. 159, 66–82. https://doi.org/10.1016/j.atmosenv.2017.03.051.

Baars, H., Ansmann, A., Engelmann, R., Althausen, D., 2008. Continuous monitoring of the boundary-layer top with lidar. Atmos. Chem. Phys. 8 (3), 10749–10790. https://doi.org/10.5194/acp-8-7281-2008.

CET, 2020a. Histórico Mês a Mês. Boletim diário de mobilidade e transportes COVID 19. http://www.cetsp.com.br/media/1096348/historico.pdf (acessed on 10th January 2020).

CET, 2020b. Mobilidade no Sistema Viário Principal. In: Volumes e Velocidades 2019. http://www.cetsp.com.br/media/1113490/msvp2019.pdf (acessed on 10th January 2020).

CETESB, 2019. Qualidade do Ar no Estado de São Paulo 2018. https://cetesb.sp.gov.br/ar/wp-content/uploads/sites/28/2019/07/Relat%C3%B3rio-de-Qualidade-do-Ar-2018.pdf (accessed on 01st June 2020).

CETESB, 2020a. QUALAR. http://cetesb.sp.gov.br/ar/qualar/ accessed on 10 June 2020).

CETESB, 2020b. Padrões de Qualidade do Ar. https://cetesb.sp.gov.br/ar/padroes-de-qualidade-do-ar/ accessed on 10th June 2020).

CETESB, 2020c. Qualidade do Ar no Estado de São Paulo 2019. https://cetesb.sp.gov.br/ar/wp-content/uploads/sites/28/2020/07/Relat%C3%B3rio-de-Qualidade-do-Ar-2019.pdf (accessed on 10th January 2021).

Collivignarelli, M.C., Abbà, A., Bertanza, G., Pedrazzani, R., Ricciardi, P., Miino, M.C., 2020. Lockdown for COVID-2019 in Milan: what are the effects on air quality? Sci. Total Environ. 732, 139280 https://doi.org/10.1016/j.scitotenv.2020.139280.

Connerton, P., Assução, J.V., Miranda, R.M., Slovic, A.D., Pérez-Martínez, P.J., Ribeiro, H., 2020. Air quality during COVID-19 in four megacities: lessons and challenges for public health. Int. J. Environ. Res. Public Health 17, 5067. https://doi.org/10.3390/ijerph17145067.

D'Amico, G., Amodeo, A., Mattis, I., Freudenthaler, V., Pappalardo, G., 2016. EARLINET single calculus chain – technical – part 1: pre-processing of raw lidar data. Atmos. Meas. Tech. 9, 491–507. https://doi.org/10.5194/amt-9-491-2016.

Dantas, G., Siciliano, B., França, B., da Silva, C.M., Arbilla, G., 2020. The impact of COVID-19 partial lockdown on the air quality of the city of Rio de Janeiro, Brazil. Sci. Total Environ. 729, 139085 https://doi.org/10.1016/j.scitotenv.2020.139085.

Debone, D., Costa, M.V., Miraglia, S.G.E.K., 2020. 90 days of COVID-19 social distancing and its impacts on air quality and health in Sao Paulo, Brazil. Sustainability 12, 7440. https://doi.org/10.3390/su12187440.

Holzworth, G.C., 1964. Estimates of mean maximum mixing depths in the contiguous United States. Mon. Wheater Rev. 92, 235–245. https://doi.org/10.1175/1520-0493(1964)092<0235:EOMMMD>2.3.CO;2.

Hynddman, R.J., Athanasopoulos, G., 2014. Forecasting: Principles and Practice. OTexts.

IBGE, 2020. Instituto Brasileiro de Geografia e Estatística. http://ibge.gov.br (accessed on 01st June 2020).

INMET, 2020. Instituto Nacional de Meteorologia. http://www.inmet.gov.br/ (accessed on 01st June 2020).

Krecl, P., Targino, A.C., Oukawa, G.Y., Junior, R.P.C., 2020. Drop in urban air pollution from COVID-19 pandemic: Policy implications for the megacity of São Paulo. Environ. Pollut. 265 (Part B), 114883. https://doi.org/10.1016/j.envpol.2020.114883.

Löning, M., Bagnall, A., Ganesh, S., Kazakov, V., Lines, J., Király, F.J., 2019. SKTIME: A Unified Interface for Machine Learning with Time Series. Pre-Print.

Moreira, G. De A., Lopes, F.J. Da S., Guerrero-Rascado, J.L., Silva, J.J., Gomes, A.A., Landulfo, E., Alados-Arboledas, L., 2019. Analyzing the atmospheric boundary layer using high-order moments obtained from multiwavelength lidar data: impact of wavelength choice. Atmos. Meas. Tech. 12 (8), 4261–4276. https://doi.org/10.5194/amt-12-4261-2019.

Moreira, G. de A., da Silva Andrade, I., Cacheffo, A., da Silva Lopes, F.J., Calzavara Yoshida, A., Gomes, A.A., da Silva, J.J., Landulfo, E., 2021. Influence of a biomass-burning event in $PM_{2.5}$ concentration and air quality: a case study in the metropolitan area of São Paulo. Sensors 21, 425. https://doi.org/10.3390/s21020425.

Moreira, G. de A., Guerrero-Rascado, J.L., Bravo-Aranda, J.A., Foyo-Moreno, I., Cazorla, A., Alados, I., Lyamani, H., Landulfo, E., Alados-Arboledas, L., 2020. Study of the planetary boundary layer height in an urban environment using a combination of microwave radiometer and ceilometer. Atmos. Res. 240, 104932. https://doi.org/10.1016/j.atmosres.2020.104932.

Nakada, L.Y.K., Urban, R.C., 2020. COVID-19 pandemic: impacts on the air quality during the partial lockdown in São Paulo state, Brazil. Sci. Total Environ. 730, 139087. https://doi.org/10.1016/j.scitotenv.2020.139087.

Otmani, A., Benchrif, A., Tahri, M., Bounakhla, M., Chakir, E.M., Bouch, M.E., Krombi, E., 2020. Impact of Covid-19 lockdown on PM_{10}, SO_2, and NO_2 concentrations in Salé City (Morocco). Sci. Total Environ. 735, 139541 https://doi.org/10.1016/j.scitotenv.2020.139541.

Paulo, São, 2013. Decreto N° 59.113, de 23 de abril de 2013. Estabelece novos padrões de qualidade do ar e dá providências correlatas. São Paulo: Assembléia Legislativa. https://cetesb.sp.gov.br/qualidade-ar/wp-content/uploads/sites/28/2013/12/decreto-59113de230413.pdf (accessed on 10th June 2020).

São Paulo Municipality, 2020. https://www.prefeitura.sp.gov.br/ (accessed on 01 June 2020).

Sharma, S., Zhang, M., Gao, J., Zhang, H., Kota, S.H., 2020. Effect of restricted emissions during COVID-19 on air quality in India. Sci. Total Environ. 728, 138878 https://doi.org/10.1016/j.scitotenv.2020.138878.

Stull, R.B., 1988. An Introduction to Boundary Layer Meteorology. Springer, Dordrecht.

Tobías, A., Carnerero, C., Reche, C., Massagué, J., Via, M., Minguillón, M.C., Alastuey, A., Querol, X., 2020. Changes in air quality during the lockdown in Barcelona (Spain) one month into the SARS-CoV-2 epidemic. Sci. Total Environ. 726, 138540. https://doi.org/10.1016/j.scitotenv.2020.138540.

Zalakeviciute, R., Vasquez, R., Bayas, D., Buenano, A., Mejia, D., Zegarra, R., Diaz, A., Lamb, B., 2020. Drastic improvements in air quality in Ecuador during the COVID-19 outbreak. Aerosol Air Qual. Res. 20, 10.4209%2Faaqr.2020.05.0254.